Journal of Engineering Physics and Thermophysics, Vol. 82, No. 5, 2009

HYDROGASDYNAMICS IN TECHNOLOGICAL PROCESSES

ANALYSIS OF THE OPERATIONAL CHARACTERISTICS OF A ROTOR-PULSATION APPARATUS WITH AN IMPELLER

A. V. Fedorov,[a] **T. A. Khmel',**[a] **M. S. Vasilishin,**[b]
A. G. Karpov,[b] **and A. A. Kukhlenko**[b]

UDC 532.695

Experimental and theoretical studies of the characteristics of a rotor-pulsation apparatus equipped with an impeller and a flow-regulating valve have been made. The dependences of the operating parameters of the apparatus on the rotor rotation frequency at four fixed positions of the valve have been determined. It has been shown that the experimental dependences of pressure in the discharge line and of net power on the number of rotations of the motor fully agree with the theoretical description from the viewpoint of the previously developed semiempirical model of the rotor-pulsation apparatus.

Keywords: *rotor-pulsation apparatus, head-flow characteristics, experiment, calculation.*

Introduction. The use of rotor-pulsation apparatuses (RPA) is a promising and effective method for extracting useful components from vegetable raw materials in the pharmaceutical industry. Various aspects of the functioning and the hydrodynamical features of the flows inside rotor-pulsation apparatuses were studied in [1–7]. In [8, 9], the results of experimental studies of an RPA designed for comminuting substrates of vegetable origin and intensifying the extraction processes are presented. The specific feature of the investigated apparatus is its equipment with an impeller and a flow regulator. Such a type of design differs from those considered in [6, 7] where the flow characteristics were only determined by the rotational velocity of the rotor and the rheological properties of the working substance.

The physico-mathematical model for describing the flows inside the device was also developed in [8, 9]. In [8], by averaging the basic mathematical model of the medium motion over the internal volume of the device, an equation for the mean velocity close to that presented in [2, 3] was obtained. In [9], the closing relations of the given model are presented, empirical constants were obtained, and a theoretical analysis of the main hydrodynamic and energy characteristics of the RPA was carried out. The calculated curves obtained from the points of view of the model are in good agreement with the experimental data of [8, 9], which made it possible to verify the model for a certain set of flow parameters.

Note that measurements of the hydrodynamic and energy characteristics were made in [9] at given values of the flow rate. In so doing, the position of the flow-regulating valve was not fixed and the minimum flow section was not determined. The experimental values of the pressure in the discharge line and the powers are given in [9] in the form of dependences on the flow rate at four different values of the synchronous rotational velocity of the RPA rotor (number of rotations). We failed to establish the relationship between the flow rate and the rotational velocity of the rotor at a fixed value of the flow section of the valve. Therefore, the theoretical analysis was restricted to a certain domain of variability of the inlet parameters of the device.

In the present work, we analyze the results of the subsequent experimental studies made at a fixed value of the flow section area of the valve, which permits redetermining the limits of the predicted mathematical model. The experimental dependences of the pressure in the discharge line, the flow rate, and net power on the motor velocity at four different positions of the valve are presented. The theoretical analysis of the new experimental data is carried out

---

[a]S. A. Khristianovich Institute of Theoretical and Applied Mechanics, Siberian Branch of the Russian Academy of Sciences, 4/1 Institutskaya Str., Novosibirsk, 630090, Russia; email: fedorov@itam.nsc.ru; [b]Institute for Problems of chemical-energy technologies, Siberian branch of the Russian Academy of Sciences, Biisk, Russia. Translated from Inzhenerno-Fizicheskii Zhurnal, Vol. 82, No. 5, pp. 823–829, September–October, 2009. Original article submitted November 3, 2008.

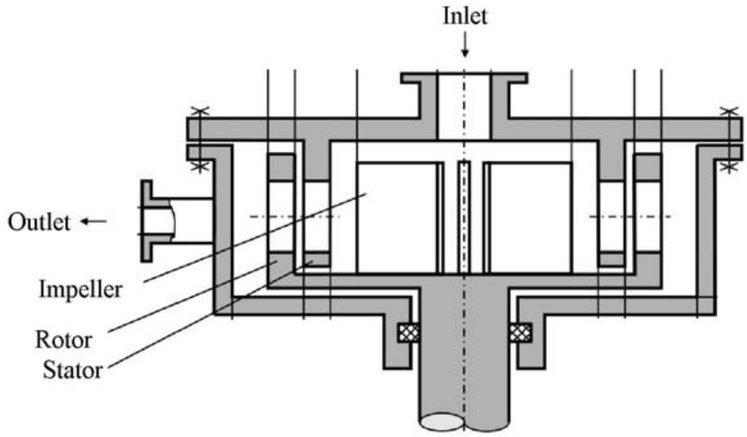

Fig. 1. Schematical representation of the device with one stator–rotor stage.

TABLE 1. Parameters of the Working Part of the Two-Stage RPA

Parameters	Stator		Rotor	
	internal	external	internal	external
Inner diameter, mm	114	142	128	156
Outer diameter, mm	124	152	138	166
Number of ducts	15	40	15	40
Width of ducts, mm	10	5	10	5
Height of ducts, mm	15	16	16	15

from the point of view of the semiempirical model presented in [9]. Comparison of calculated and experimental data has made it possible to widen the field of application of the model of [9].

Experimental. A detailed description is given in [9]. For completeness, we give the description of the basic units and the characteristic features of the functioning of a two-stage RPA (the section of one stage is schematically represented in Fig. 1). The working substance is fed into the device through the central inlet duct and is swirled by the impeller vanes, then it passes through the ducts of the stators and rotors and is removed through the outlet. The impeller contains six vanes of length 29 mm, peripheral height of 17 mm, and inner diameter 50 mm. The diameters of the inlet and outlet pipes are, respectively, 32 and 27 mm. The stator and rotor stages represent hollow cylinders with rectangular ducts on the side surface. The geometric characteristics of the stator and rotor are presented in Table 1. The duct width and length were measured in the azimuthal and axial direction, respectively. During the operation of the apparatus the relative position of the stator and rotor ducts and, accordingly, the flow section vary continuously, i.e., the flow in the apparatus is pulsating.

Because in using highly inflammable liquids as an extractant there exist certain restrictions on the transportation velocity, the apparatus is equipped with a valve (regulator) for a smooth change in the flow rate. The valve is located behind the outlet duct immediately ahead of the flowmeter. The pressure in the discharge line was measured by a manometer placed between the outlet duct and the valve. The pressure at the RPA inlet (inlet line) in all experiments was constant. The schematic representation of the liquid circulation loop and designations of the main units are given in [9].

The electric power consumed by the motor was measured by means of two wattmeters with "triangle"-type connection of motor windings. The mechanical power on the motor shaft (net power) was calculated with account for the known dependence of the efficiency on the power consumption by the formula $N = \xi N_{el}$.

Table 2 presents the results of four sets of experiments at a fixed position of the valve (i.e., for four different values of the flow section of the valve) in the form of measured pressure values in the discharge line and the flow rate, as well as calculated values of mechanical power. The results are also given graphically in Figs. 2–4 where the curve number corresponds to the number of the set of experiments. Note that the measurement data are charac-

TABLE 2. Experimental Characteristics of the RPA

Characteristics	Ω, rpm								
	600	900	1200	1500	1800	2100	2400	2700	3000
Set 1, S = 0.36 cm²									
P_{dis}, MPa	0.012	0.025	0.042	0.060	0.090	0.115	0.148	0.185	0.225
Q, m³/h	0	0.3	0.5	0.7	0.85	0.95	1.1	1.2	1.4
N, W	61	179	256	382	455	520	911	1188	1599
Set 2, S = 1.22 cm²									
P_{dis}, MPa	0.012	0.022	0.040	0.057	0.090	0.106	0.140	0.170	0.205
Q, m³/h	0.6	0.95	1.4	1.7	2.00	2.50	2.80	3.10	3.50
N, W	45	150	256	346	455	554	958	1204	1714
Set 3, S = 2.12 cm²									
P_{dis}, MPa	0.011	0.021	0.035	0.052	0.072	0.095	0.122	0.153	0.186
Q, m³/h	1.0	1.6	2.3	3.0	3.7	4.4	5.1	5.8	6.4
N, W	45	100	225	346	421	589	1007	1308	2144
Set 4, S = 3.80 cm²									
P_{dis}, MPa	0.011	0.0175	0.028	0.040	0.052	0.065	0.085	0.100	0.160
Q, m³/h	1.65	3.0	4.4	6.0	7.6	9.4	11.4	13.6	16.0
N, W	45	124	256	458	690	1000	1497	1999	–

terized by a small spread, which permits elucidating certain mechanisms in the correlation dependences of characteristic parameters.

Theoretical Analysis of the Experimental Data. *Head-flow characteristics.* Let us give the basic formulas for calculating the RPA characteristics in accordance with the hydrodynamics model proposed in [8, 9]. The relation between the flow rate and the characteristic transportation velocity is defined in the form $U = Q/(2\pi RZ)$, where Z is the length of the ducts of stators and rotors (size in the axial direction). According to the analysis of the time dependence of the transportation velocity performed in [9], velocity fluctuations can be neglected at mean transportation velocity values less than 0.025. Estimates of the experimental data from Table 2 show that the above value of the dimensionless transportation velocity is not obtained in sets 1–3 ($S_{valve} \le 2.12$ cm^2) and partly in experiments of set 4 ($S_{valve} = 3.80$ cm^2) at flow rate values less than 8 m^3/h, i.e., in most cases in the given set of experiments one can use a model neglecting the pulsating character of the flow in calculating the basic characteristics of the apparatus.

In accordance with the scheme used, the pressure in the discharge line is composed of the inlet pressure, the head provided by the rotation of the vanes and the rotor minus the pressure losses due to the internal drag of the RPA and the losses in the transition parts (inlet duct, outlet duct):

$$P_{dis} = P_{inlet} + P_{imp} + P_{rot} - \Delta P_{int} - \Delta P_{inlet} - \Delta P_{out} + 0.5\rho\left(U_{inlet}^2 - U_{dis}^2\right). \tag{1}$$

Here each term is defined as follows. The statistical component of the pressure at the point of liquid inlet to the RPA $P_{inlet} = 0.01$ MPa. The head created by the centrifugal force of the liquid mass involved in the rotation by the impeller vanes $P_{imp} = \vartheta_{imp}\rho(2\pi\Omega)^2(R_{imp,outer}^2 - R_{imp,in}^2)$. The efficiency coefficient of the impeller ϑ_{imp} was determined in [9] by comparing the calculated and experimental data at various values of the flow rate and the number of motor rotations. The empirical value of the coefficient varies from 0.76 (at very low transportation velocities) to 0.68. The head provided by the rotation of the rotor stages is defined as $P_{rot} = 0.4\rho(2\pi\Omega)^2RH$ (at $H \ll R$). The coefficient 0.4 expresses the ratio of the total area of the rotor ducts to the side surface of the rotor since the centrifugal force is only created by the liquid mass present in the ducts of the device. The internal pressure losses $\Delta P_{int} = \rho c_{int}U^2/2$, where c_{int} is the time-average value of the internal drag of the stator–rotor system. The pressure losses at the inlet to the device with account for the involvement of the liquid in the rotation are presumably defined as follows: $\Delta P_{inlet} \approx \rho\vartheta_{inlet}U_{inlet}^2/2$, where $\vartheta_{inlet} < 1$ ([10], p. 146–147). As before, we neglect these losses ($\vartheta_{inlet} \ll 1$). The losses at the liquid inlet to the outlet duct due to the narrowing of the flow section are taken in the form $\Delta P_{out} = 0.5(1 - S_{out}/(2\pi RZ))\rho U_{out}^2/2$ ([10], p. 151). Taking into account the smallness of the output duct area, we can approximately assume $\Delta P_{out} \approx 0.25\rho U_{out}^2 = 0.25(2\pi RZ/S_{out})^2\rho U^2$.

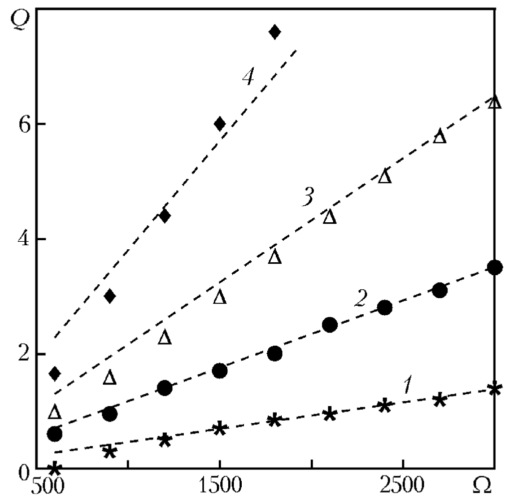

Fig. 2. Flow rate of the liquid as a function of the number of motor rotations. Q, m^3/h; Ω, rpm.

Determination of the Flow Rate. Suppose that for the liquid circulation loop the Bernoulli equation holds (this assumption is in accord with the experimental data of both [9] and the present work). Then, taking into account the pressure losses on the regulating valve and the additional pressure losses in the line $\Delta P_{\text{valve}} = \rho c_{\text{valve}} U_{\text{out}}^2/2$, $\Delta P_{\text{ad}} = \rho c_{\text{ad}} U_{\text{out}}^2/2$, we have

$$P_{\text{dis}} + 0.5\rho U_{\text{out}}^2 - \Delta P_{\text{valve}} - \Delta P_{\text{ad}} = P_{\text{inlet}} + 0.5\rho U_{\text{inlet}}^2 . \tag{2}$$

Taking into account the dependences of the transportation velocity in different sections on the flow rate (measured characteristics) $U = Q/(2\pi RZ)$, $U_{\text{out}} = Q/S_{\text{out}}$, $U_{\text{inlet}} = Q/S_{\text{inlet}}$, from (1)–(2) we obtain

$$Q = 2\pi\Omega \sqrt{\frac{\vartheta_{\text{imp}} \left(R_{\text{imp,outer}}^2 - R_{\text{imp,in}}^2\right) + 0.4RH}{0.5c_{\text{int}}/(2\pi RZ)^2 + 0.5\,(0.5 + c_{\text{ad}})/S_{\text{out}}^2 + 0.5c_{\text{valve}}/S_{\text{valve}}^2}} . \tag{3}$$

For each run of measurements (at a fixed position of the value) c_{valve} is constant. As was shown earlier, the quantities c_{int} and ϑ_{imp} can be considered to be constant except for the domain of small values of the flow rate. Then the expression under the root is a constant and thus the linear dependence of the flow rate on the number of motor rotations is determined. In Fig. 2, dots show the experimental values of Q as a function of the rotational velocity of the rotors, and dashed lines present the calculation by formula (3). As is seen, the data of the sets of experiments 1 and 2 (at small values of the transition cross-section on the valve) are in good agreement with the theoretical curves. In the sets of experiments 3 and 4, the slight deviation from the linear dependence is likely due to the following two factors. First, at such a significant amplitude of the change in the flow rate with increasing number of rotations the quantity ϑ_{imp} can no longer be considered to be constant. Second, at large values of the flow rate and relatively low rotational velocities of the rotor the pressure losses at the inlet duct increase and, consequently, they can probably be neglected. Note that to the operating conditions there corresponds the region of $\Omega > 1000$ rpm and $\Omega < 5.4$ m^3/h [9]. It is seen from Fig. 2 that in this region the experimental points fall fairly well on the theoretical straight lines.

The linear dependence of the flow rate on the number of motor rotations also agrees with the experimental data [6]. The approximating dependences are given in [6] in the form $Q = \alpha\Omega - Q_*$, where the quantity Q_* is related to the existence of the upthrust regime in the hydrotract, the reasons for whose existence are not explained. Note that the data for vegetable oil presented in the figure at $3000 < \Omega < 5000$ rpm also fall well (within the limits of the spread) on the straight line passing through the origin of coordinates, i.e., correspond to the dependence of the form (3).

Pressure in the Discharge Line. In view of the obtained dependence of the flow rate on the number of motor rotations the dependence of the discharge pressure on the flow rate is determined from (2) as follows:

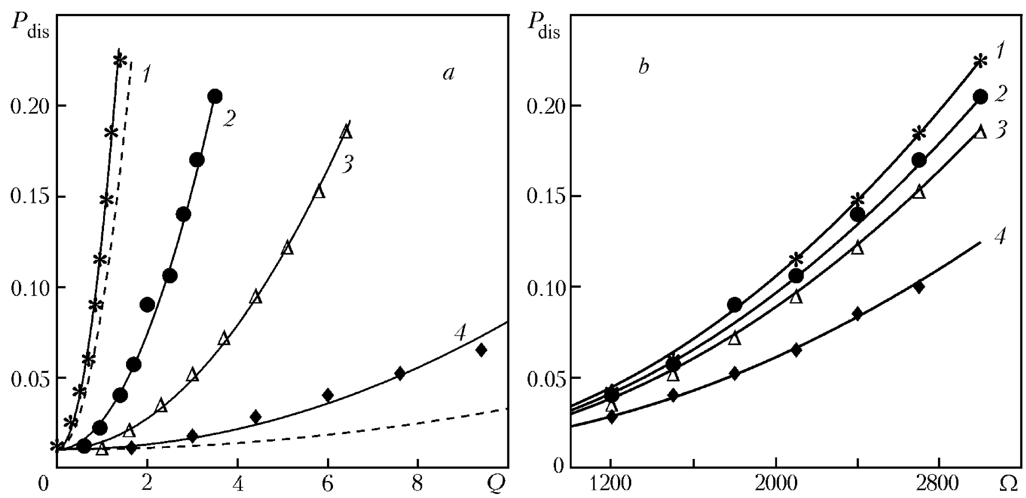

Fig. 3. Pressure in the discharge line as a function the flow rate (a) and the number of motor rotations (b). P_{dis}, MPa; Q, m^3/h; Ω, rpm.

$$P_{\text{dis}} = P_{\text{inlet}} + 0.5\rho\left(\frac{Q}{2\pi RZ}\right)^2\left(\frac{1}{\sigma_{\text{inlet}}^2} + \frac{c_{\text{valve}} + c_{\text{ad}} - 1}{\sigma_{\text{out}}^2}\right), \tag{4}$$

where P_{inlet} = 0.01 MPa; $\sigma = S/(2\pi RZ)$ is the contraction coefficient of a part of the device. In Fig. 3a, solid lines show the calculated dependences (4) obtained at values of the quantity $c_{\text{valve}} + c_{\text{ad}}$ that best agrees with the experimental data. Dashed lines present the calculated curves obtained at c_{ad} = 0 and the estimated value of c_{valve} determined in [9] by the formula

$$c_{\text{valve}} = \frac{[0.707\,(1-\sigma_{\text{valve}})^{0.375} + 1 - \sigma_{\text{valve}}]^2}{(\sigma_{\text{out}}\sigma_{\text{valve}})^2}, \quad \sigma_{\text{valve}} = \frac{S_{\text{valve}}}{S_{\text{out}}}, \tag{5}$$

corresponding to the drag in flowing past lattices or in flowing through a hole with thin edges [10, p. 152]. As is seen, the parabolic dependence of the discharge pressure on the flow rate agrees with experiments, which confirms again the correctness of the ideas about the proceeding processes taken by us earlier. The slight discrepancy between the calculated data determined by formula (5) and the experimental data (dots) may be due to the following reasons. First, errors in measuring the flow section of the valve lead to a significant error in determining the drag coefficient. Second, formula (5) is given in [9] as an estimating formula since the configurations of the flows inside the structure of the regulating valve and through holes or lattices are different. Here, as in [9], the calculated RPA characteristics are determined from the point of view of the semiempirical model and are based on experimental data.

From formulas (4) and (3) we can also determine the parabolic dependences of the discharge pressure on the number of motor rotations. As is seen from Fig. 3b, the experimental values (dots) fall well on these curves (solid lines).

Power Characteristics. The net power is determined by the following formula [9]:

$$N = N_0 + N_{\text{imp}} + N_{\text{rot}} + N_{\text{tr}}\,. \tag{6}$$

Here N_0 is the power expended in the rotation of rotors and vanes at a zero flow rate; N_{imp} and N_{rot} are the powers expended in swirling the liquid flowing between the vanes and in the rotor holes; N_{tr} is the power expended in overcoming the drag forces in the process of liquid transportation (internal drag in the RPA, drag on the inlet and outlet ducts, and the drag on the regulating valve). The quantity $N_0 = A_0\Omega^3$ includes the shut-off capacity of the electric motor and the power expended in overcoming the moment of resistance in the process of rotation of the vanes and the

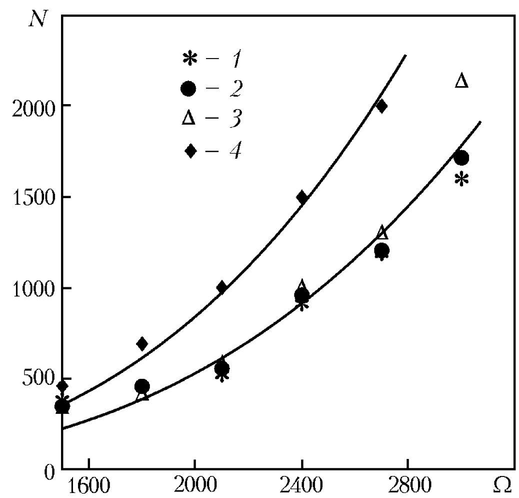

Fig. 4. Motor power as a function of the rotation frequency of the rotor. N, W; Ω, rpm.

rotor. The power expended in swirling the inflowing liquid by the impeller vanes and in the rotor ducts was determined in [9] as

$$N_{\text{imp}} + N_{\text{rot}} = \rho\,(2\pi\Omega)^2\,Q\left(\eta_{\text{imp}} R^2_{\text{imp,outer}} + 2\eta_{\text{rot}} R^2\right), \tag{7}$$

where η_{imp}, η_{rot} are coefficients reflecting the degree of involvement in the rotation of the liquid flowing through the impeller vanes and the rotor ducts.

The power expended in overcoming all drag forces in the process of liquid transportation, with account for the applicability of the Bernoulli theorem to the conditions at the inlet to and outlet from the device, is

$$N_{\text{tr}} \approx (P_{\text{imp}} + P_{\text{rot}})\,Q = \rho\,(2\pi\Omega)^2\,Q\left[\vartheta_{\text{imp}}\left(R^2_{\text{imp,outer}} - R^2_{\text{imp,in}}\right) + 0.4RH\right]. \tag{8}$$

The cubic dependence of power on Ω at a zero flow rate (N_0) and the linear dependence on the flow rate at a fixed rotational velocity of the rotor (7)–(8) are confirmed by the experimental data presented by us earlier in [9].

Taking into account the linear dependence of the flow rate on the number of rotations at a fixed position of the valve, which is given by formula (3), the total power from (7)–(8) is given by a cubic function of the number of rotations. In Fig. 4, this dependence is shown by solid lines, and dots represent the experimental data in the 1200–3000 rpm range.

It should be noted that the spread in power values is very small at a fixed rotational velocity of the rotor and with a varying flow section of the regulating valve in the sets of experiments in 1–3. This is likely due to the relatively weak influence of some of the terms connected with the flow rate, in particular, of the portion of energy expended in involving the inflowing liquid in the rotation on the impeller vanes and in the rotors. In set 4 (at a completely open valve) this portion markedly increases, which shows up as a noticeable increase in the power.

Conclusions. We have made experimental and theoretical studies of the operational characteristics of a rotor-pulsation apparatus with an impeller and a flow rate limiter at fixed values of the flow section on the valve.

The experimental dependences of pressure in the discharge line and of net power on the number of rotations fully agree with the theoretical data obtained from the viewpoint of the semiempirical RPA model developed in [9]. It should be noted that:

1) the dependences of the flow rate Q on the number of motor rotations Ω in the domain of parameters corresponding to the operating conditions ($Q < 5.4$ m^3/h, $\Omega > 1200$ rpm) are linear functions;

2) the pressure in the discharge lines depends quadratically on the flow rate and the number of motor rotations with the corresponding proportionality coefficients depending on the geometric and design characteristics of the RPA;

3) the dependence of net power on the number of rotations at a fixed position of the valve is a cubic function; a weak dependence on the flow section area of the valve has been noted in the sets of experiments 1–3, i.e., within the range of variability of the section up to 60% of its total value.

NOTATION

A, coefficient in the linear dependence; c, drag coefficient; H, depth of ducts, m; N, power, W; P, pressure, head, MPa; Q, flow rate, m^3/sec; R, radius, m; S, flow section, m^2; U, transportation velocity, m/sec; Z, length of ducts; α, coefficient in the linear dependence; ρ, density, kg/m^3; σ, contraction coefficient of the flow section; ϑ, efficiency coefficient; η, coefficient of involvement in rotation; ξ, motor efficiency; Ω, rotation frequency of the rotor, 1/sec. Subscripts: 0, at a zero flow rate; 1, 2, internal and external in the stator–rotor system; max, maximum; valve, valve; in, internal for the impeller; int, internal for the device; inlet, inlet duct; out, outlet duct; ad, additional; imp, impeller; outer, outer for the impeller; dis, in the discharge line; rot, rotor; ave, average in the stator–rotor system; tr, transportation; el, electric.

REFERENCES

1. M. A. Promtov, *Machines and Apparatuses with Impulse Power Actions on Treated Substances* [in Russian], Mashinostroenie, Moscow (2004).
2. A. I. Zimin, *Applied Mechanics of Intermittent Flows* [in Russian], Foliant, Moscow (1997).
3. A. M. Balabyshko, A. I. Zimin, and V. P. Ruzhitskii, *Hydromechanical Dispersion* [in Russian], Nauka, Moscow (1998).
4. A. I. Nakorchevskii, B. I. Basok, and T. S. Ryzhkova, Hydromechanics of rotory-pulsation apparatuses, *Inzh.-Fiz. Zh.*, **75**, No. 2, 58–68 (2002).
5. T. V. Sorokina, Hydrodynamic instability in rotory-pulsation apparatuses, *Prom. Teplotekh.*, **26**, No. 6, 80–82 (2004).
6. I. A. Pirozhenko, Experimental investigations of thermal and hydrodynamic characteristics of a fluid in a rotory-pulsation apparatus, *Prom. Teplotekh.*, **26**, No. 6, 106–113 (2004).
7. Yu. S. Kravchenko, B. I. Basok, B. V. Davydenko, and I. A. Pirozhenko, Influence of the viscosity of a treated medium on the dynamic characteristics of a rotory-pulsation apparatus, *Prom. Teplotekh.*, **26**, No. 1, 7–11 (2004).
8. Yu. A. Gosteev, A. V. Fedorov, V. M. Fomin, and T. A. Khmel', *On Two Problems of the Mechanics of Heterogeneous Media* [in Russian], Preprint No. 3-2006 of the S. A. Khristianovich Institute of Theoretical and Applied Mechanics, Siberian Branch of the Russian Academy of Sciences, Novosibirsk (2006).
9. V. M. Fomin, A. V. Fedorov, T. A. Khmel', M. S. Vasilishin, A. G. Karpov, and A. A. Kukhlenko, Theoretical and experimental investigation of the characteristics of a rotor-pulsation apparatus, *Inzh.-Fiz. Zh.*, **81**, No. 5, 817–825 (2008).
10. I. E. Idel'chik, *Handbook on Hydrodynamic Resistances* [in Russian], Mashinostroenie, Moscow (1992).